Title

Developmental and molecular contributions to contextual fear memory emergence in mice

Authors

Alexandra L. Lanjewar, Ph.D.[1,2,3], Pat Levitt, Ph.D.[1,2], Kathie L. Eagleson, Ph.D.[1,2]

Affiliations

[1]Program in Developmental Neuroscience and Neurogenetics, Children's Hospital Los Angeles, The Saban Research Institute, Los Angeles, CA, United States. [2]Department of Pediatrics, Keck School of Medicine of University of Southern California, Los Angeles, CA, United States. [3]Corresponding author: 4650 Sunset Blvd. Los Angeles, CA 90027, 323-361-7868, alanjewar@chla.usc.edu

ABSTRACT

Cognitive impairment is a common phenotype of neurodevelopmental disorders, but how these deficits arise remains elusive. Determining the onset of discrete cognitive capabilities facilitates studies in probing mechanisms underlying their emergence. The present study analyzed the emergence of contextual fear memory persistence (7-day memory retention) and remote memory (30-day memory retention). There was a rapid transition from postnatal day (P) 20 to P21, in which memory persistence emerged in C57Bl/6J male and female mice. Remote memory was present at P23, but expression was not robust compared to pubertal and adult mice. To address a potential molecular mechanism, the present study examined the MET receptor tyrosine kinase (MET), which when deleted results in fear memory deficits in adult mice and regulates timing of critical period in the visual cortex, positioning it as a regulator for onset of contextual fear memory. Sustaining *Met* past the normal window of peak cortical expression or deleting *Met* did not alter the timing of emergence of persistence or remote memory capabilities. However, failure to exhibit fear memory occurred by P90 in mice with reduction or deletion of *Met*. Remarkably, the number of FOS-expressing infragranular neurons in medial prefrontal cortex (mPFC) did not increase with contextual conditioning at P35 but exhibited enhanced activation at P90. Additionally, MET-expressing neurons were preferentially recruited at P90 compared to P35 during fear memory expression. The studies demonstrate a developmental profile of contextual fear memory capabilities. Further, developmental disruption of *Met* leads to a delayed functional deficit that arises in adulthood.

INTRODUCTION

Cognitive development is a protracted process, and brain regions involved, such as medial prefrontal cortex (mPFC), continue to mature into early adulthood [1-5], coinciding with increased and optimized cognitive capacity [6-8]. Cognitive deficits are common in neurodevelopmental disorders (NDDs) [9-15]; however, how and when such deficits arise remain elusive.

In rodents, contextual fear paradigms are used to assess learning and memory functions. Perturbations in the expression of NDD risk genes during development can lead to contextual fear deficits in mice. Most studies, however, focus analyses on adults [16-18], leaving a knowledge gap in the temporal and mechanistic origins of cognitive deficits. Studies have begun to focus on the normative ontology of contextual fear learning abilities in wild type mice. As early as postnatal day (P) 15, mice form a fear memory that lasts at least 1-day (d) but does not persist for 7-d [19]. By P25, longer-term memory capabilities are present, such that mice can retain fear memories for at least 30-d [20]. These studies identify a broad window of cognitive development, during which longer-term memory capabilities arise. The precise trajectory, however, remains unknown.

Accumulating evidence underscores a key role for the MET receptor tyrosine kinase (MET) in the development of discrete circuits within the forebrain. In cortex, abundant MET expression coincides with the period of peak synaptogenesis, and MET signaling modulates dendritic and synapse development and maturation [21-26]. Prolonging or

eliminating MET expression alters the timing of critical period plasticity for ocular dominance, shifting the critical period later or earlier, respectively [24]. Additionally, prolonging MET expression during a critical period for social cognition alters social behavior in adult mice [25]. Finally, adult mice in which *Met* had been conditionally deleted embryonically in all neural cells or in cells arising from the dorsal pallium only exhibit contextual fear learning deficits [27-29]. Thus far, no study has determined when these deficits arise. Together, these studies position MET as a candidate for regulating the timing of onset for contextual fear memory capabilities.

Here, we determine the precise developmental trajectory for onset of 7-d persistent memory capabilities and whether this coincides with the onset of remote memory capabilities (30-d memory) [30-31]. We also determine whether sustaining or eliminating MET signaling affects contextual fear memory abilities prior to adulthood. Lastly, experiments were performed to determine the developmental and adult activity of MET^{+} neurons in mPFC during contextual fear memory.

MATERIALS AND METHODS

Animals

Mice were bred in the Children's Hospital Los Angeles (CHLA) vivarium and housed on ventilated racks with a 13:11 hour light:dark cycle at 22°C with ad libitum access to water and a standard chow diet (PicoLab Rodent Diet 20, #5053, St. Louis, MO). All mouse lines were maintained on a C57Bl6/J background. Therefore, the C57Bl/6J strain (The Jackson Laboratory) was used as the wild type (WT) mouse line to determine the

normal developmental trajectory for retaining a 7-d persistent memory or a 30-d remote memory. To sustain MET expression in all dorsal pallial excitatory neurons, a controllable transgenic overexpression for *Met* (cto-*Met*) mouse line was used, as previously described [25]. In this line, the *Met* transgene is expressed abundantly by P16 [24] and sustained throughout the course of experiments. Littermates not expressing the *Met* transgene were considered controls. To delete the *Met* gene, $Met^{fx/fx}$ females and $Nestin^{cre}$; $Met^{fx/+}$ males were bred to produce control (Cre-negative), conditional heterozygous (cHet; $Nestin^{cre}/Met^{fx/+}$), and conditional homozygous (cKO; $Nestin^{cre}/Met^{fx/fx}$) pups [27]. The cHet mice produce 50% of normal MET levels and the cKO mice do not produce any MET in neural cells. Lastly, a Met^{EGFP} BAC transgenic mouse line was used to visualize green fluorescent protein (GFP) in MET-expressing neurons in mice homozygous for the *Met-EGFP* transgene (Met^{GFP}), as previously described [32-33]. For all mice, the day of birth was designated P0. At P21 (+/-1 d), mice were weaned and housed with same-sex littermates (2-5/cage). To minimize potential litter and sex effects, each experimental group included a maximum of 2 males and 2 females from a single litter, with a minimum of three litters and approximately equal numbers of males and females represented. For all analyses, investigators were blind to genotype and condition. Animal care and experiments conformed to the guidelines set forth by the CHLA Institutional Animal Care and Use Committee.

Contextual Fear Conditioning and Testing

Contextual fear conditioning and memory testing were performed as described in Akers et al. [19] (Fig. 1A) using the NIR Video Fear Conditioning Package for Mouse (MED-

VFC2-USB-M; Med Associates Inc, Georgia, VT). Fear conditioning chambers (Med Associates VFC-008-LP) were 29.53x23.5x20.96cm with shock-grid floors (Med Associates VFC-005A). Shocks were generated by a standalone aversive stimulator/scrambler (Med Associates ENV-414S). Separate cohorts of mice from each mouse line were trained on P15, P20, P21, P22, P23, P35, P46-P53 (post-pubertal adolescents, denoted P50 from hereon) or P89-P99 (adults, denoted P90 from hereon). Briefly, “Shock” mice were acclimated in the chamber for 2-min and then presented with 3 unsignaled 2-sec foot shocks of 0.5mA intensity spaced 1-min apart. One minute after the last shock, mice were removed from the chamber and returned to their home cage. Shock delivery was confirmed by mice jumping and/or vocalizing during the shock. In the instances that shock delivery could not be confirmed for all three shocks, mice were excluded from further testing (<5%); there were no age, sex, or genotype differences in exclusions. Age-matched littermates designated “No-Shock” mice were placed in the chamber for the same length of time without receiving foot shocks and served as controls for spontaneous (non-memory induced) freezing. Memory trials were conducted 1- (formation), 7- (persistence), 14- (longer persistence), or 30- (remote) d later. On the testing day, mice were returned to the chamber and allowed to explore for 5-min (or 2-min in FOS experiments) without any foot shocks presented.

Behavioral Analysis

During testing day, freezing responses were recorded by a monochrome video camera (Med Associates VID-CAM-MONO-5). A freeze response was considered no movement above an 18au threshold for at least 1-sec (30 frames), analyzed by automated

software (Video Freeze, SOF-843, Med Associates). The percentage of time freezing over the 5-min (or 2-min) trial on testing day was calculated by the automated software.

Immunohistochemistry Staining

At P36 or P91, 90-min after contextual fear memory formation testing, *Met*^{GFP} brains were collected, processed, and immunostained as previously described [34]. The primary antibodies (1:500) used were chicken anti-GFP (Abcam Cat#ab13970, RRID:AB_300798), rat anti-CTIP2 (Abcam Cat#ab18465, RRID:AB_2064130), and rabbit anti-CFOS (Cell Signaling Technology Cat#2250, RRID:AB_2247211). Alexa Fluor® F(ab')$_2$ conjugated secondary antibodies (1:500; Abcam) were used.

Imaging and Cell Count Analysis

Sections including mPFC (corresponding to areas 24a, 25, and 32 [35]) were imaged on a Zeiss LSM 700 inverted confocal microscope using a 20×/0.8NA Plan-APOCHROMAT objective lens with refractive index correction. 2µm z-stacks were acquired through the entire thickness of the section at 1AU (0.313x0.313x2µm). Three brain sections, at least 100µm apart, were imaged, counted, and averaged per animal. Manual counts were performed using the 'cell counter' plugin in FIJI software version 2.9.0 (https://fiji.sc/, RRID:SCR_002285). Images were cropped by layer based on CTIP2 immunostaining and DAPI, so that they could be analyzed in a layer-specific manner. The width of the cortical crop was held constant (321µm), while the thickness varied to capture the full depth of each layer. The total number of DAPI nuclei, FOS$^+$ cells and GFP$^+$ cells, as well as FOS$^+$; GFP$^+$ double-labeled cells, were counted. The

marker of interest was considered a positive count only if there was both immunofluorescence signal and a $DAPI^+$ nucleus.

Statistical Analyses

Data are reported as mean ± standard error of the mean to the second decimal place. Sample sizes are reported in the figures. An individual animal represents a single sample. Sample sizes were determined using a power analysis at α=0.05 and 1-β=0.8 (SPH Analytics, statistical power calculator using average values). For all analyses, test statistics are reported to the second decimal place and *p* values are reported to the fourth decimal place. Statistical analyses were performed using GraphPad Prism software version 9.1.2 (GraphPad Software, Inc, La Jolla, CA). For each statistical analysis, a D'Agostino & Pearson normality test ($n \geq 8$) or a Shapiro-Wilk normality test ($n < 8$), was performed. One-tailed Mann-Whitney (non-parametric; test statistic: *U*), Kruskal-Wallis (non-parametric; test statistic: *H*), followed by a post hoc Dunn's multiple comparisons test if omnibus test detected a significant difference, two-tailed unpaired *t*-tests (parametric; test statistic: *t*), ordinary one-way ANOVA (parametric; test statistic: *F*), followed by a post hoc Tukey multiple comparisons tests if omnibus test detected a significant difference, Kolmogorov-Smirnov (non-parametric; test statistic *D*), and two-way ANOVA, followed by Šídák's multiple comparisons test, were used.

RESULTS

To determine the precise developmental onset of contextual fear memory persistence capabilities in WT mice, Shock mice at different developmental ages were conditioned

and tested 7-d later. Freezing responses on testing day were compared to age-matched No-Shock mice. Contextual fear memory persistence capabilities were considered present when the Shock group exhibited significantly increased freezing responses compared to the No-Shock group. There was no significant difference in percentage time freezing between the Shock (1.65 ± 1.05) and No-Shock (0.56 ± 0.34) groups 7-d after training on P15 (U = 26.00; p = 0.4168; Fig. 1B), contrasting with the significant differences observed in mice trained on P35 (U = 1.00; p < 0.0001; No-Shock: 0.44 ± 0.16; Shock: 16.92 ± 4.80; Fig. 1C). These results demonstrate that the ability to retain a contextual fear memory for at least 7-d emerges between P15-P35 in C57BL/6J mice, consistent with the previous report in a mixed background strain [19].

We next trained separate cohorts of mice at various ages between P15-P35, testing for persistent memory. For mice trained on P20, the Shock group (2.80 ± 1.56) exhibited no significant difference in percentage time freezing compared to the No-Shock group (0.68 ± 0.14; U = 22.00; p = 0.4242; Fig. 1D). Remarkably, when mice were trained 1-d later (P21), a significant difference between the two groups was observed (U = 0; p < 0.0001; No-Shock: 0.09 ± 0.05; Shock: 23.08 ± 6.87; Fig. 1E). There was no effect of age on the freezing response in the No-Shock group between P21-P35 (H = 3.20; p = 0.3614; P21: 0.09 ± 0.05; P22: 1.43 ± 0.98; P23: 0.46 ± 0.32; P35: 0.44 ± 0.16; Fig. 1F), demonstrating no differences in spontaneous freezing due to age. Therefore, we next compared freezing responses in the Shock group across these ages. There was no significant age effect in percentage time freezing (H = 6.61; p = 0.0854; P21: 23.08 ± 6.87; P22: 29.08 ± 7.43; P23: 31.97 ± 6.94; P35: 16.92 ± 4.80; Fig. 1G), indicating no

further maturation of persistent memory expression over the two weeks following onset. Together, these data show rapid onset of contextual fear memory persistence capabilities at P21, with comparable memory expression as older ages.

Remote contextual fear memory capabilities are present at P25 but not at P21 in WT mice using a 5-shock paradigm [20]. We determined whether remote fear memory is present within this timeframe using our 3-shock paradigm. Thirty days following training at P23, one of the earliest ages that contextual fear memory persistent capabilities are present, there was a significant increase in percentage time freezing in Shock (7.05 $\pm$ 2.24) compared to No-Shock (0.02 $\pm$ 0.02; $U = 28$; $p < 0.0001$; Fig. 2A) mice. Because the freezing response appeared blunted compared to that observed after the 7-d training-testing interval (Fig. 1G), we measured the freezing response of Shock mice at different training-testing intervals (7-, 14-, 30-d). Mice trained at P23 exhibited a significant effect of training-testing interval on percentage time freezing ($H = 14.73$; $p = 0.0006$; Fig. 2B), driven by a significant difference between the 7-d (31.97 $\pm$ 6.94) and 30-d (7.05 $\pm$ 2.24) intervals ($p = 0.0004$). All other post-hoc comparisons were not significant. Thus, P23 mice exhibit blunted remote fear memory expression compared to memory persistence, while 14-d memory retention resulted in intermediate fear expression (15.34 $\pm$ 4.26). In contrast, there was no training-testing interval effect when mice were trained on P35 ($H = 1.83$; $p = 0.3998$; 7-d: 16.92 $\pm$ 4.80; 14-d: 28.92 $\pm$ 6.78; 30-d: 18.98 $\pm$ 5.08; Fig. 2C), demonstrating that at P35, memory expression is as robust for remote memory as for shorter intervals of memory expression.

MET protein in cortex begins downregulating around P21 in mice and is greatly reduced by P35 [21]. With the developmental trajectories for persistent and remote memories defined and coinciding temporally with MET downregulation, we next tested the hypothesis that downregulation of MET expression in the cortex is necessary for emergence of contextual fear memory persistence and remote memory during development. Separate cohorts of cto-*Met* (sustained MET expression) and littermate control mice were trained between P23-P90 and tested 7- or 30-d later. Since there were no genotype differences found at any age in the No-Shock mice (data not shown), only genotype effects between age-matched Shock mice were compared. There was no difference between control (32.75 $\pm$ 4.19) and cto-*Met* (32.39 $\pm$ 7.10) Shock mice in percentage time freezing for those trained on P23, one of the earliest ages that memory persistence is present in WT mice, and tested 7-d later (t = 0.05; p = 0.9640; Fig. 3A). Next, P35 mice, an age at which there is robust remote memory expression in WT mice (Fig. 2C), were tested for remote memory. Remote memory was intact, with no difference between control (23.69 $\pm$ 5.97) and cto-*Met* (21.01 $\pm$ 5.59) Shock mice in percentage time freezing on testing day (t = 0.33; p = 0.7480; Fig. 3B). Together, these data indicate that downregulation of MET expression is not required for emergence of contextual fear memory persistence or remote memory capabilities. Lastly, we determined there was no difference between P90 control (18.46 $\pm$ 4.06) and cto-*Met* (14.20 $\pm$ 3.65) Shock mice in percentage time freezing on testing day 7-d later (t = 0.78; p = 0.4448; Fig. 3C), indicating downregulation of MET is not necessary for memory persistence capabilities in adulthood.

We next probed when the previously reported adult contextual fear deficits first arise in the *Nestin*-cre; *Met*^{fx} line [27-28]. We first confirmed a significant genotype effect at P90 on percentage time freezing in Shock mice tested 1-d later *(F* = 6.82; *p* = 0.0034), with cHet (2.53 ± 1.16) and cKO (4.14 ± 1.17) mice exhibiting reduced freezing compared to the control group (11.99 ± 2.18; control vs cHet: *p* = 0.0127; control vs. cKO: *p* = 0.0127; Fig. 4A), demonstrating the 3-shock paradigm used in the current study was sufficient to induce memory formation deficits in adult mice. Remarkably, there was no effect of genotype on percentage time freezing 1-d (*F* = 0.23; *p* = 0.7440; control: 35.10 ± 5.9414; cHet: 37.82 ± 6.05; cKO: 30.78 ± 7.39; Fig. 4B) and 7-d (*H* = 0.92; *p* = 0.6477; control: 35.38 ± 4.32; cHet: 32.24 ± 5.43; cKO: 44.83 ± 12.80; Fig. 4C) following training on P23. Similarly, there was no effect of genotype on percentage time freezing in mice tested for remote memory 30-d after training on P35 *(H* = 4.63; *p* = 0.0989; control: 17.05 ± 3.77; cHet: 12.51 ± 4.40; cKO: 9.07 ± 3.14; Fig. 4D) or on ~P50 (post-pubertal adolescence [36]; *H* = 2.95; *p* = 0.2286; control: 11.23 ± 4.18; cHet: 8.31 ± 3.64; 6.09 ± 3.05; Fig. 4E). Together, these data demonstrate adult-specific deficits in contextual fear memory following elimination of *Met* in neural cells.

mPFC contributes to contextual fear memory circuitry [37-38], and MET is enriched in subcerebral projection neurons in infragranular layers of mPFC throughout postnatal development in mice [39]. We hypothesized that age-dependent differences in the MET population could contribute to the observed adult-specific deficit in fear memory. We first determined if there were differences in the percentage of MET-expressing cells at P35 compared to adult mice. Analyses using the *Met*^{GFP} line to visualize GFP in *Met*-

expressing cells (Fig. 5A) revealed no significant difference in MET-GFP cell density in layer 5 (P35: 15.59 ± 0.58; P90: 17.61 ± 1.13; t = 1.50; p = 0.1691; Fig. 5B) or layer 6 (P35: 14.04 ± 1.00; P90: 8.85 ± 1.78; D = 0.67; p = 0.1429; Fig. 5C). We next probed whether there were age differences in the percentage of MET cells that are activated during memory expression. Mice were conditioned on P35 or P90 and tested 1-d later. Memory-induced FOS^+ cells were quantified and compared to baseline levels of FOS in age-matched mice that remained in their home cage. Importantly, there was no significant difference in freezing responses during 1-d memory testing between P35 (22.63 ± 6.72) and P90 (13.64 ± 2.84), demonstrating that fear expression behavior is comparable at both ages (D = 0.50; p = 0.4740; Fig. 5D). We first considered the FOS-expressing population independent of MET expression. Two-way ANOVA revealed a main effect of age (p = 0.0268) and condition (memory-tested versus home-cage; p = 0.0043), but no interaction effect (p = 0.1391) on the percentage of FOS cells in layer 5 (Fig. 5E). Unexpectedly, post-hoc analyses revealed no significant difference in percentage of FOS cells between memory-tested (21.51 ± 1.68) and home-caged (15.40 ± 3.73; p = 0.4453) mice at P35, contrasting with the significantly higher percentage of FOS cells in memory-tested (35.69 ± 5.66; p = 0.0051) compared to home-caged (18.48 ± 1.63) mice at P90. In layer 6 mPFC, two-way ANOVA revealed a main effect of condition (p = 0.0020), but no age effect (p = 0.4196) or interaction (p = 0.0812; Fig. 5F). Again, post-hoc analyses revealed no significant difference in percentage of FOS cells between home-caged (12.44 ± 1.89) and memory (16.81 ± 1.44; p = 0.4223) mice at P35, in contrast to a significantly higher percentage of FOS cells in memory-tested (23.59 ± 4.17; p = 0.0022) compared to home-caged (9.86 ±

1.73) mice at P90. Together, these results indicate that cells in infragranular mPFC are preferentially engaged during memory expression at P90, but not P35, compared to baseline. Finally, we quantified the percentage of FOS-expressing MET-GFP cells in mPFC at P35 and P90 during 1-d memory expression (Fig. 5G). There was a significant increase in FOS^{+}; GFP^{+} cells, normalized to total FOS, at P90 compared to P35 in layer 5 (P35: 28.98 $\pm$ 1.67, P90: 48.85 $\pm$ 4.23; t = 4.37 p = 0.0014; Fig. 5H) and layer 6 (P35: 21.84 $\pm$ 1.38, P90: 46.11 $\pm$ 4.66; D = 1.00; p = 0.0022; Fig. I). These data indicate that MET-GFP cells in mPFC are preferentially recruited during 1-d fear memory expression in adults, but not at P35.

DISCUSSION

The present study provides a new understanding of the temporal profile for the acquisition of memory capabilities in developing mice. The abrupt onset of memory persistence between P20-P21 occurs after mice can retain a memory for 1-d but prior to having the capacity for fully expressed remote memory. This is independent of weaning, as shifting weaning a day earlier or later had no impact on the onset of contextual fear memory persistence (data not shown). Interestingly, in contrast to memory persistence, remote memory becomes fully expressed gradually over the days following initial onset. Together, these data indicate that longer-term memory capabilities develop in a stepwise fashion, first with emergence of shorter-term abilities that mature into longer-term capabilities over time. The current findings provide a necessary temporal framework for future studies probing the mechanisms that underlie these transitions and for determining biological and environmental factors that accelerate or delay this

trajectory. The data also identify a potential sensitive period in memory development, during which disruptions in the maturational processes that allow this cognitive function to become fully expressed would have a profound impact on learning and memory capabilities.

Based, in part, on the correlation between the timing of MET expression downregulation in the cortex and the onset of contextual fear memory persistence, we focused on a potential role for MET in the development of this cognitive capacity. Contrary to expectations, an “off” signal of *Met* is not necessary for normal contextual fear memory development or adult expression. Further, while *Met* expression is necessary for contextual fear memory in adults, embryonic deletion or reduction of *Met* had no impact on contextual fear memory expression through the late adolescent period. These findings were similar to behavioral deficits observed in adult, but not juvenile, mice that were haploinsufficient in *Myt1l*, a gene highly expressed early postnatally but not in adults [40]. In both instances, reduction in normal protein expression leads to the emergence of some behavioral deficits only after circuit maturation is complete, well beyond the period of normal peak protein expression. Our finding of increased activation of infragranular mPFC neurons during 1-d memory expression compared to baseline at P90, but not P35, support a greater reliance on engaging mPFC circuitry for memory expression in adults compared to the early adolescent period. Consistent with this, inactivation of mPFC after conditioning in post-weanling rats does not affect 1-d memory expression [41]. We suggest that adolescence represents a second sensitive period, during which fear memory capabilities are present but the underlying brain

circuits recruited are different than in adults. If, during this period, circuits subserving adult fear memory do not develop properly, for example due to reduction of *Met* expression, deficits may arise as this cognitive function becomes more dependent upon mPFC involvement. Major pruning in mPFC projections to the basal amygdala, connectivity that is involved in adult fear memory circuitry, occurs between P45-P90 [42]. This period of refinement represents a time during which circuitry is vulnerable and, if disrupted, could lead to adult-specific deficits.

While *MET* was initially considered an autism spectrum disorder (ASD) risk gene, with reduced expression found in temporal cortex in ASD and Rett Syndrome [43-46], it more likely serves as an important receptor for modulating the maturation of subsets of synapses in the developing cerebral cortex, leading to circuit development vulnerabilities if signaling is disrupted. Studies of MET function in the cortex has therefore largely been studied in a developmental context. The adult-onset deficits in fear memory formation observed in *Met* null mice could, however, reflect a previously unrecognized adult-specific function of MET. Indeed, the findings that MET expression is enriched in the FOS^{+} cells in infragranular mPFC during the expression of fear memory in adults compared to adolescents, even though the percentage of MET-GFP expressing cells is the same, indicate an adult-specific engagement of MET-expressing cells in mPFC during fear memory expression. Because cortical neurons with sustained MET expression have more biochemically immature synaptic properties [24], adult expression of MET may maintain subsets of synapses in a more plastic state during adult learning and memory.

The present study advances insight into the precise timing of the ontology of contextual fear memory capabilities, facilitating the design of additional studies to determine the molecular mechanisms involved in the onset and continued expression of this cognitive function into adulthood. Additionally, the finding that not all functional deficits observed in adults are expressed during development emphasizes the need for careful temporal analyses of the timing onset of functional disturbances. Experimental data that precisely define typical development trajectories of additional cognitive abilities would further benefit studies aiming to address mechanisms underlying neurodevelopmental disorders and the cognitive deficits that are often associated with them. This study focused on contextual fear memory, and thus, does not exclude MET from having roles in regulating the onset of other cognitive functions and the timing of distinct critical periods. We also note that while the present study focused on mPFC, other brain regions may also contribute to the observed adult deficits when *Met* is conditionally deleted. Future studies will address the impact of modulating neuronal activity of neuronal subtypes expressing MET in mPFC on contextual fear memory in adults, as well as on other cognitive assays across development.

ACKNOWLEDGEMENTS

We thank Amanda Whipple for assistance with animal husbandry and genotyping. We thank Dr. Allison Knoll and Miranda Villanueva for technical assistance in setting up the contextual fear memory chambers and paradigms. Lastly, we thank Dr. Esteban

Fernandez of the Cellular Imaging Core at The Saban Research Institute (TSRI), Children's Hospital Los Angeles for assistance with image acquisition and analysis.

AUTHOR CONTRIBUTIONS

All authors contributed to conceiving and designing the research. A.L.L. performed the experiments and analyses. All authors interpreted the data. A.L.L. drafted the manuscript. All authors revised the manuscript for important intellectual content. All authors approved the final version to be published. All authors agree to be accountable for all aspects of the work.

FUNDING

This work was supported by National Institute of Mental Health R01 MH067842, TSRI Developmental Neuroscience and Neurogenetics Program Simms/Mann Chair in Developmental Neurogenetics and the WM Keck Chair in Neurogenetics.

COMPETING INTERESTS

The authors have nothing to disclose.

REFERENCES

1. Calabro FJ, Murty VP, Jalbrzikowski M, Tervo-Clemmens B, Luna B. Development of hippocampal-prefrontal cortex interactions through adolescence. Cereb Cortex. 2020;30:1548-58.
2. Gogtay N, Giedd JN, Lusk L, Hayashi KM, Greenstein D, Vaituzis AC, et al. Dynamic mapping of human cortical development during childhood through early adulthood. Proc Natl Acad Sci U S A. 2004;101:8174-9.
3. Shaw P, Kabani NJ, Lerch JP, Eckstrand K, Lenroot R, Gogtay N, et al. Neurodevelopmental trajectories of the human cerebral cortex. J Neurosci. 2008;28:3586-94.
4. Sowell ER, Thompson PM, Holmes CJ, Jernigan TL, Toga AW. In vivo evidence for post-adolescent brain maturation in frontal and striatal regions. Nat Neurosci. 1999;2:859-61.
5. Mills KL, Lalonde F, Clasen LS, Giedd JN, Blakemore SJ. Developmental changes in the structure of the social brain in late childhood and adolescence. Soc Cogn Affect Neurosci. 2014;9:123-31.
6. Best JR, Miller PH, Naglieri JA. Relations between executive function and academic achievement from ages 5 to 17 in a large, representative national sample. Learn Individ Differ. 2011;21:327-36.
7. Luna B, Garver KE, Urban TA, Lazar NA, Sweeney JA. Maturation of cognitive processes from late childhood to adulthood. Child Dev. 2004;75:1357-72.

8. Luciana M, Conklin HM, Hooper CJ, Yarger RS. The development of nonverbal working memory and executive control processes in adolescents. Child Dev. 2005;76:697-712.
9. Reichenberg A, Caspi A, Harrington H, Houts R, Keefe RS, Murray RM, et al. Static and dynamic cognitive deficits in childhood preceding adult schizophrenia: A 30-year study. Am J Psychiatry. 2010;167:160-9.
10. Kahn RS, Keefe RS. Schizophrenia is a cognitive illness: Time for a change in focus. JAMA Psychiatry. 2013;70:1107-12.
11. Keefe RS, Eesley CE, Poe MP. Defining a cognitive function decrement in schizophrenia. Biol Psychiatry. 2005;57:688-91.
12. Cantio C, White S, Madsen GF, Bilenberg N, Jepsen J. Do cognitive deficits persist into adolescence in autism?. Autism Res. 2018;11:1229-38.
13. Damaj L, Lupien-Meilleur A, Lortie A, Riou É, Ospina LH, Gagnon L, et al. CACNA1A haploinsufficiency causes cognitive impairment, autism and epileptic encephalopathy with mild cerebellar symptoms. Eur J Hum Genet. 2015;23:1505-12.
14. Kallweit C, Paucke M, Strauß M, Exner C. Cognitive deficits and psychosocial functioning in adult ADHD: Bridging the gap between objective test measures and subjective reports. J Clin Exp Neuropsychol. 2020;42:569-83.
15. Loyer Carbonneau M, Demers M, Bigras M, Guay MC. Meta-analysis of sex differences in ADHD symptoms and associated cognitive deficits. J Atten Disord. 2021;25:1640-56.

16. Nakamoto C, Kawamura M, Nakatsukasa E, Natsume R, Takao K, Watanabe M, et al. GluD1 knockout mice with a pure C57BL/6N background show impaired fear memory, social interaction, and enhanced depressive-like behavior. PLoS One 2020;15:e0229288.
17. Haji N, Riebe I, Aguilar-Valles A, Artinian J, Laplante I, Lacaille JC. Tsc1 haploinsufficiency in Nkx2.1 cells upregulates hippocampal interneuron mTORC1 activity, impairs pyramidal cell synaptic inhibition, and alters contextual fear discrimination and spatial working memory in mice. Mol Autism. 2020;11:29.
18. Huang L, Wang J, Liang G, Gao Y, Jin SY, Hu J, et al. Upregulated NMDAR-mediated GABAergic transmission underlies autistic-like deficits in *Htr3a* knockout mice. Theranostics. 2021;11:9296-310.
19. Akers KG, Arruda-Carvalho M, Josselyn SA, Frankland PW. Ontogeny of contextual fear memory formation, specificity, and persistence in mice. Learn Mem. 2012;19:598-604.
20. Samifanni R, Zhao M, Cruz-Sanchez A, Satheesh A, Mumtaz U, Arruda-Carvalho M. Developmental emergence of persistent memory for contextual and auditory fear in mice. Learn Mem. 2021;28:414-21.
21. Judson MC, Bergman MY, Campbell DB, Eagleson KL, Levitt P. Dynamic gene and protein expression patterns of the autism-associated MET receptor tyrosine kinase in the developing mouse forebrain. J Comp Neurol. 2009;513:511-31.
22. Judson MC, Eagleson KL, Wang L, Levitt P. Evidence of cell-nonautonomous changes in dendrite and dendritic spine morphology in the MET-signaling-deficient mouse forebrain. J Comp Neurol. 2010;518:4463-78.

23. Eagleson KL, Lane CJ, McFadyen-Ketchum L, Solak S, Wu HH, Levitt P. Distinct intracellular signaling mediates C-MET regulation of dendritic growth and synaptogenesis. Dev Neurobiol. 2016;76:1160-81.
24. Chen K, Ma X, Nehme A, Wei J, Cui Y, Cui Y, et al. Time-delimited signaling of MET receptor tyrosine kinase regulates cortical circuit development and critical period plasticity. Mol Psychiatry. 2021;26:3723-36.
25. Ma X, Wei J, Cui Y, Xia B, Zhang L, Nehme A, et al. Disrupted timing of MET signaling derails the developmental maturation of cortical circuits and leads to altered behavior in mice. Cereb Cortex. 2022;32:1769-86.
26. Xie Z, Eagleson KL, Wu HH, Levitt P. Hepatocyte growth factor modulates MET receptor tyrosine kinase and β-catenin functional interactions to enhance synapse formation. eNeuro. 2016;3:ENEURO.0074-16.2016.
27. Thompson BL, Levitt P. Complete or partial reduction of the Met receptor tyrosine kinase in distinct circuits differentially impacts mouse behavior. J Neurodev Disord. 2015;7:35.
28. Heun-Johnson H, Levitt P. Differential impact of *Met* receptor gene interaction with early-life stress on neuronal morphology and behavior in mice. Neurobiol Stress. 2017;8:10-20.
29. Xia B, Wei J, Ma X, Nehme A, Liong K, Cui Y, et al. Conditional knockout of MET receptor tyrosine kinase in cortical excitatory neurons leads to enhanced learning and memory in young adult mice but early cognitive decline in older adult mice. Neurobiol Learn Mem. 2021;179:107397.

30. Frankland PW, Ding HK, Takahashi E, Suzuki A, Kida S, Silva AJ. Stability of recent and remote contextual fear memory. Learn Mem. 2006;13:451-7.
31. Silva BA, Burns AM, Gräff J. A cFos activation map of remote fear memory attenuation. Psychopharmacology. 2019;236:369-81.
32. Kamitakahara A, Wu HH, Levitt P. Distinct projection targets define subpopulations of mouse brainstem vagal neurons that express the autism-associated MET receptor tyrosine kinase. J Comp Neurol. 2017;18:3787-808.
33. Kast RJ, Wu HH, Levitt P. Developmental connectivity and molecular phenotypes of unique cortical projection neurons that express a synapse-associated receptor tyrosine kinase. Cereb Cortex, 2019;29:189-201.
34. Kast RJ, Lanjewar AL, Smith CD, Levitt P. Foxp2 exhibits projection neuron class specific expression, but is not required for multiple aspects of cortical histogenesis. eLife. 2019;8:e42012.
35. Paxinos G, Franklin KB. Paxinos and Franklin's the mouse brain in stereotaxic coordinates - electronic. 5th ed. Elsevier - OHCE; 2019
36. Plochocki JH. Mechanically-induced osteogenesis in the cortical bone of pre- to peripubertal stage and peri- to postpubertal stage mice. J Orthop Surg Res. 2009;4:22.
37. Stevenson CW. Role of amygdala-prefrontal cortex circuitry in regulating the expression of contextual fear memory. Neurobiol Learn Mem. 2011;96:315-23.
38. Maren S, Phan KL, Liberzon I. The contextual brain: Implications for fear conditioning, extinction and psychopathology. Nat Rev Neurosci. 2013;14:417-28.

39. Lanjewar AL, Jagetia S, Khan ZM, Eagleson KL, Levitt P. Subclass-specific expression patterns of MET receptor tyrosine kinase during development in medial prefrontal and visual cortices. J Comp Neurol. 2023;531:132-48.
40. Kim S, Oh H, Choi SH, Yoo YE, Noh YW, Cho Y, et al. Postnatal age-differential ASD-like transcriptomic, synaptic, and behavioral deficits in Myt1l-mutant mice. Cell Rep. 2022;40:111398.
41. Awad W, Kritman M, Ferreira G, Maroun M. Differential recruitment of the infralimbic cortex in recent and remote retrieval and extinction of aversive memory in post-weanling rats. Int J Neuropsychopharmacol. 2022;25:489-97.
42. Cressman VL, Balaban J, Steinfeld S, Shemyakin A, Graham P, Parisot N, et al. Prefrontal cortical inputs to the basal amygdala undergo pruning during late adolescence in the rat. J Comp Neurol. 2010;518:2693-709.
43. Campbell DB, Sutcliffe JS, Ebert PJ, Militerni R, Bravaccio C, Trillo S, et al. A genetic variant that disrupts MET transcription is associated with autism. Proc Natl Acad Sci U S A. 2006;103:16834-39.
44. Campbell DB, D'Oronzio R, Garbett K, Ebert PJ, Mirnics K, Levitt P, et al. Disruption of cerebral cortex MET signaling in autism spectrum disorder. Ann Neurol. 2007;62:243-50.
45. Plummer JT, Evgrafov OV, Bergman MY, Friez M, Haiman CA, Levitt P, et al. Transcriptional regulation of the MET receptor tyrosine kinase gene by MeCP2 and sex-specific expression in autism and Rett syndrome. Transl Psychiatry. 2013;3:e316.

46. Aldinger KA, Timms AE, MacDonald JW, McNamara HK, Herstein JS, Bammler TK, et al. Transcriptome data of temporal and cingulate cortex in the Rett syndrome brain. Sci Data. 2020;7:192.

FIGURE LEGENDS

Fig. 1: Contextual fear memory persistence rapidly emerges at P21 in WT mice.

A Diagram of contextual fear memory persistence paradigm used in the present study. **B** Quantification of the percentage time freezing on testing day of No Shock (n = 7) and Shock (n = 8) mice trained on P15 and tested 7 d later. The Shock group did not exhibit significantly more freezing than the No Shock mice. **C** Quantification of the percentage time freezing on testing day of No Shock (n = 14) and Shock (n = 15) mice trained on P35 and tested 7 d later. The Shock group exhibited significantly more freezing than No Shock (****$p < .0001$). **D** Quantification of the percentage time freezing on testing day of No Shock (n = 6) and Shock (n = 8) mice trained on P20 and tested 7 d later. The Shock group did not exhibit significantly more freezing than the No Shock mice. **E** Quantification of the percentage time freezing on testing day of No Shock (n = 12) and Shock (n = 13) mice trained on P21 and tested 7 d later. The Shock group exhibited significantly more freezing than No Shock (****$p < .0001$). **F** Quantification of the percentage time freezing on testing day of No Shock mice trained at different ages and tested 7 d later (P21: n = 12; P22: n = 10; P23: n = 6; P35: n = 14). No significant difference across age was determined. **G** Quantification of the percentage time freezing on testing day of Shock mice trained at different ages and tested 7 d later (P21: n = 13; P22: n = 11; P23: n = 10; P35: n = 15). No significant difference across age was determined.

Fig. 2: Traces of remote contextual fear memory are present at P23 but is still developing compared to P35.

A Quantification of the percentage time freezing on testing day of No Shock (n = 17) and Shock (n = 18) mice trained on P23 and tested 30 d later. The Shock group exhibited significantly more freezing than No Shock (****$p < .0001$). **B** Quantification of the percentage time freezing on testing day of Shock mice conditioned on P23 and tested 7 (n = 10), 14 (n = 8), or 30 (n = 18) d later. There is a significant difference between 1 and 30 d training intervals (***$p < .001$). **C** Quantification of the percentage time freezing on testing day of Shock mice conditioned on P35 and tested 7 (n = 15), 14 (n = 11), or 30 (n = 9) d later. There is no significant difference across training intervals.

Fig. 3: Sustaining MET past its normal temporal peak in the cortex does not affect contextual fear memory persistence developmentally or in adulthood.

A Quantification of the percentage time freezing on testing day of control (n = 23) and cto-*Met* (n = 10) genotypes of Shock mice conditioned on P23 and tested 7 d later. No significant difference between genotypes was determined. **B** Quantification of the percentage time freezing on testing day of control (n = 8) and cto-*Met* (n = 8) genotypes of Shock mice conditioned on P35 and tested 30 d later. No significant difference between genotypes was determined. **C** Quantification of the percentage time freeing on testing day of control (n = 11) and cto-*Met* (n = 11) genotypes of Shock mice conditioned on P90 and tested 7 d later. No significant difference between genotype was determined.

Fig. 4: Reduction or absence of MET expression in neurons impacts contextual fear memory in adulthood but not during development.

A Quantification of the percentage time freezing on testing day of control (n = 17), cHet (n = 7), and cKO (n = 11) *Nestin*^{cre}/*Met*^{fx} Shock mice conditioned on P90 and tested 1 d later. There is a significant difference between control and cHet genotypes and control and cKO genotypes (*$p < 0.05$). **B** Quantification of the percentage time freezing on testing day of control (n = 10), cHet (n = 11), and cKO (n = 9) *Nestin*^{cre}/*Met*^{fx} Shock mice conditioned on P23 and tested 1 d later. No significant difference across genotypes was determined. **C** Quantification of the percentage time freezing on testing day of control (n = 9), cHet (n = 8), and cKO (n = 5) *Nestin*^{cre}/*Met*^{fx} Shock mice conditioned on P23 and tested 7 d later. No significant difference across genotypes was determined. **D** Quantification of the percentage time freezing on testing day of control (n = 17), cHet (n = 12), and cKO (n = 15) *Nestin*^{cre}/*Met*^{fx} Shock mice conditioned on P35 and tested 30 d later. No significant difference across genotypes was determined. **E** Quantification of the percentage time freezing on testing day of control (n = 10), cHet (n = 9), and cKO (n = 12) *Nestin*^{cre}/*Met*^{fx} Shock mice conditioned on P50 and tested 30 d later. No significant difference across genotypes was determined.

Fig. 5: MET-GFP and FOS expression in infragranular layers 5 and 6 of mPFC at P35 compared to P90.

A Exemplary images of DAPI (blue) and MET-GFP (green) in layers 5 and 6 mPFC at P35 (left) and P90 (right). Blue arrows denote DAPI nuclei, yellow arrows denote GFP$^+$ cells, scale bars = 50 µm. **B** Quantification of the percentage of MET-GFP$^+$ cells in layer 5 mPFC at P35 (n = 5) and P90 (n = 6). No significant difference between ages was determined. **C** Quantification of the percentage of MET-GFP$^+$ cells in layer 6 mPFC at

P35 (n = 6) and P90 (n = 6). No significant difference between ages was determined. **D** Quantification of the percentage time freezing of *Met*^{GFP} Shock mice conditioned on P35 (n = 6) or P90 (n = 6) and tested 1 d later. No significant difference between ages was determined. **E** Quantification of the percentage of FOS^{+} cells in layer 5 mPFC in P35 and P90 home-caged and contextual fear memory formation tested mice (P35 home-caged: n = 5; P35 memory: n = 6; P90 home-caged: n = 6; P90 memory: n = 6). There were significant age and condition effects, with a significant difference between P90 home-caged and P90 memory tested mice (*p < .05, **p < .01, ns, not significant). **F** Quantification of the percentage of FOS^{+} cells in layer 6 mPFC in P35 and P90 home-caged and contextual fear memory formation tested mice (P35 home-caged: n = 6; P35 memory: n = 6; P90 home-caged: n = 6; P90 memory: n = 6). There was a significant condition effect, with a significant difference between P90 home-caged and P90 memory tested mice (**p < .01, ns, not significant). **G** Exemplary images of FOS (magenta) and MET-GFP (green) in layers 5 and 6 mPFC at P35 (left) and P90 (right). Blue arrows denote FOS^{+} cells, yellow arrows denote FOS^{+};GFP^{+} colocalized cells, scale bars = 50 µm. **H** Quantification of the percentage of FOS^{+};GFP^{+} colocalized cells out of total FOS-expressing cells in layer 5 mPFC in mice conditioned on P35 (n = 6) or P90 (n = 6) and tested 1 d later and in layer 6 mPFC (**I**). There was a significant difference between ages in both layers (**p < .01).

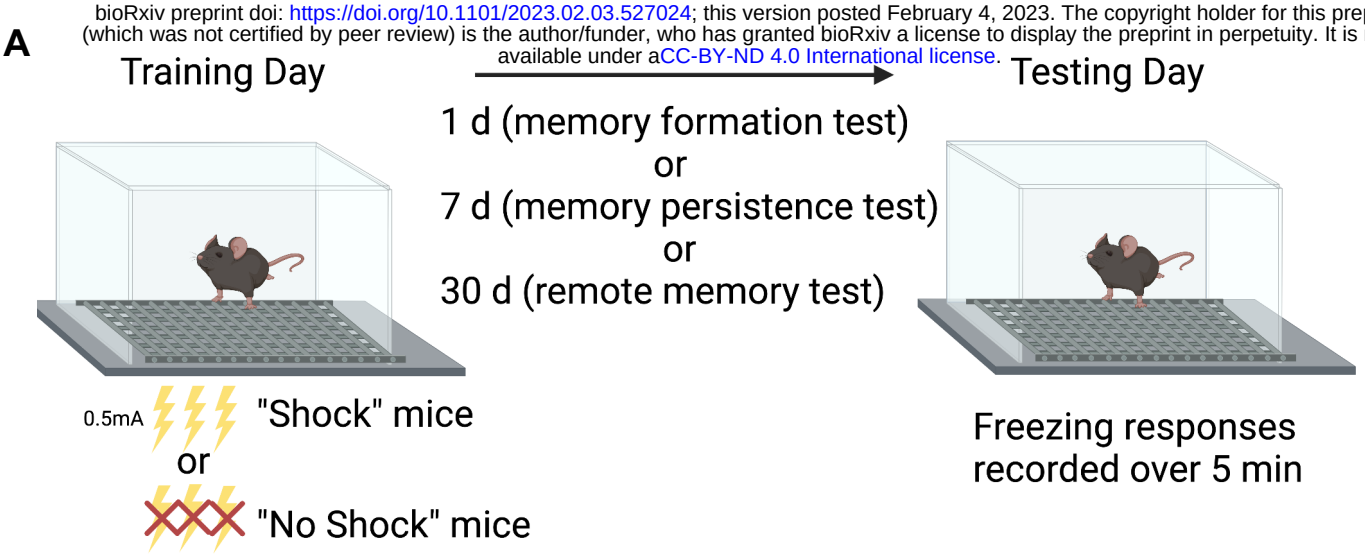

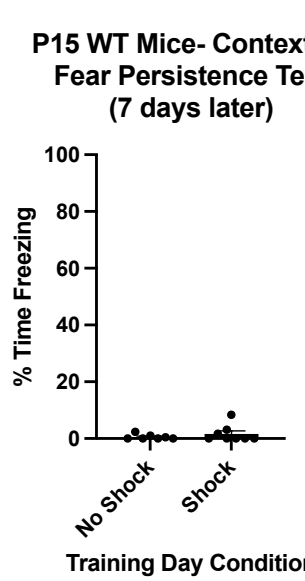

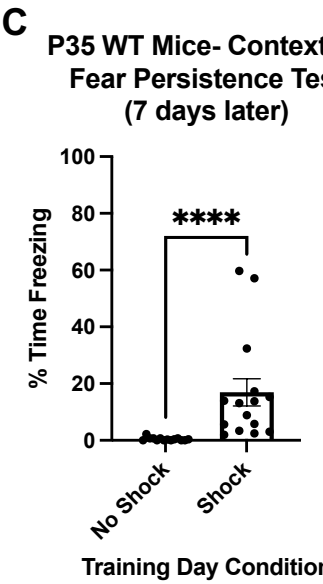

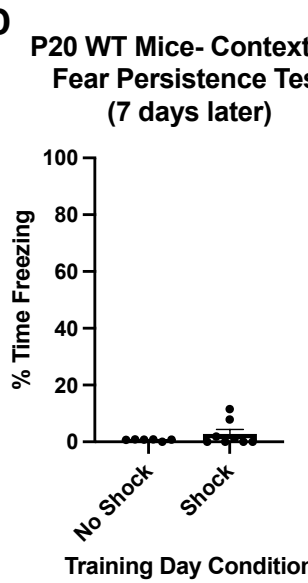

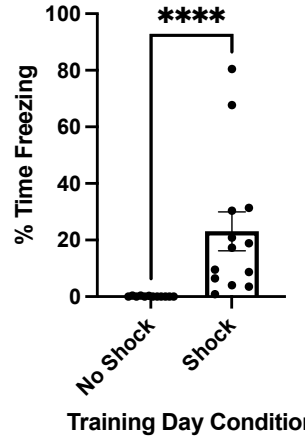

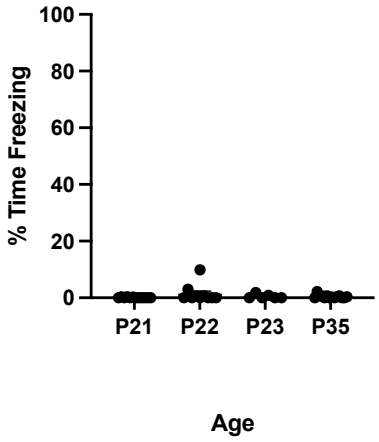

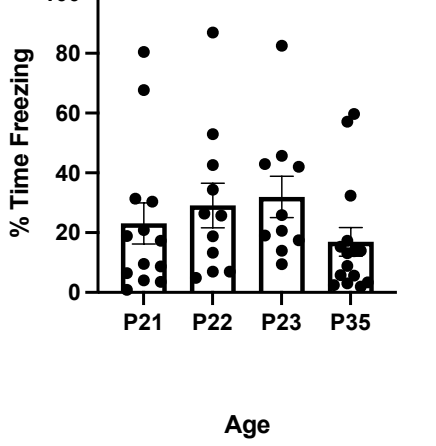

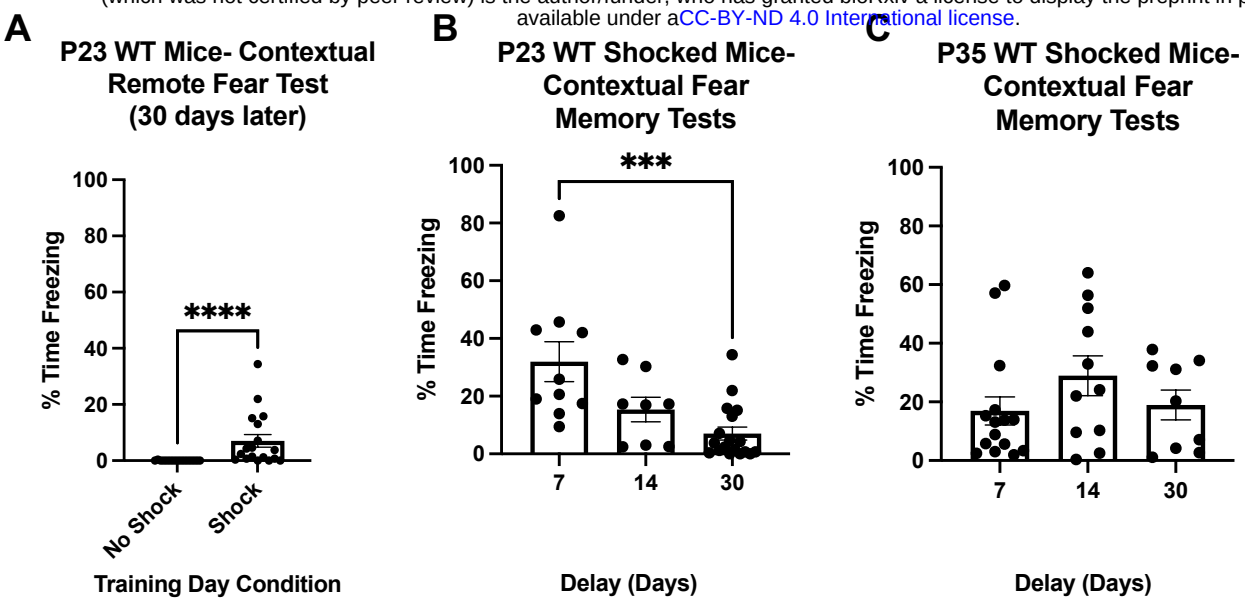

A

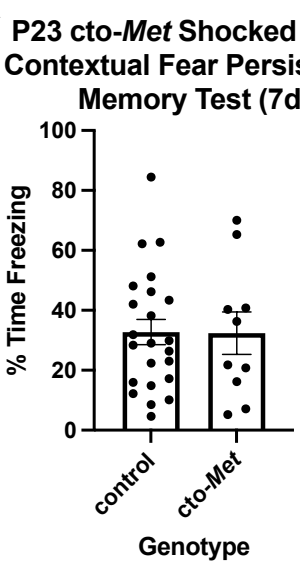

B

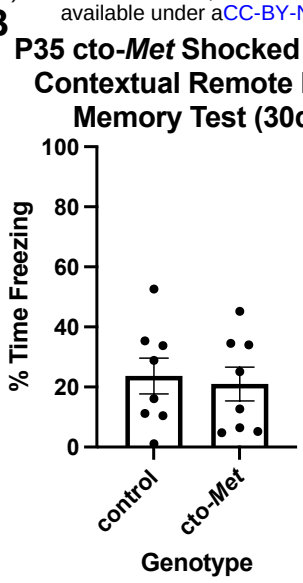

C

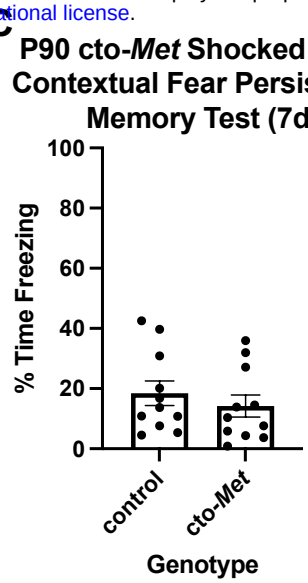

A

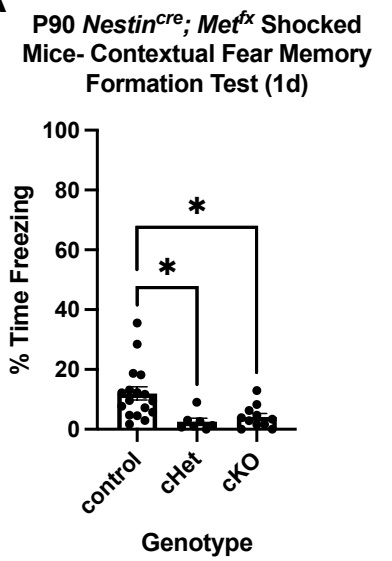

B

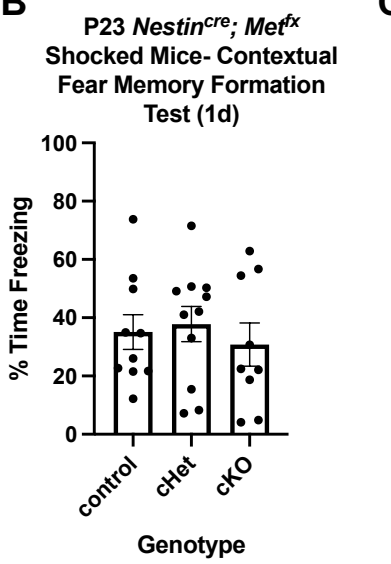

C

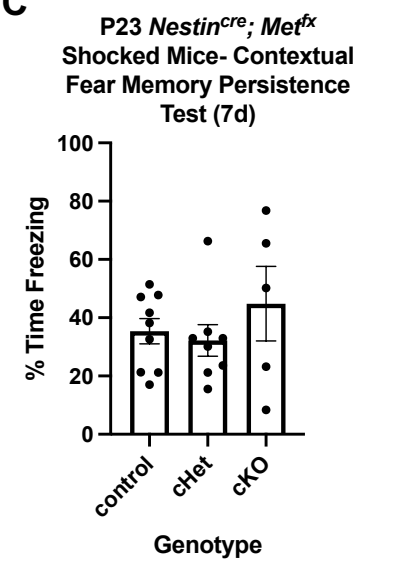

D

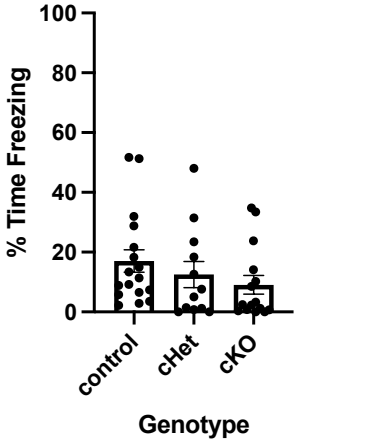

E